AIP Journal of Applied Physics

Phase shift multiplication effect of all-optical analog to electromagnetically induced transparency in two micro-cavities side coupled to a waveguide system

Boyun Wang, Tao Wang, Jian Tang, Xiaoming Li, and Chuanbo Dong

Citation: Journal of Applied Physics **115**, 023101 (2014); doi: 10.1063/1.4861128
View online: http://dx.doi.org/10.1063/1.4861128
View Table of Contents: http://scitation.aip.org/content/aip/journal/jap/115/2?ver=pdfcov
Published by the AIP Publishing

JOURNAL OF APPLIED PHYSICS **115**, 023101 (2014)

Phase shift multiplication effect of all-optical analog to electromagnetically induced transparency in two micro-cavities side coupled to a waveguide system

Boyun Wang, Tao Wang,[a)] Jian Tang, Xiaoming Li, and Chuanbo Dong
Wuhan National Laboratory for Optoelectronics, Huazhong University of Science and Technology, Wuhan 430074, China

(Received 28 September 2013; accepted 16 December 2013; published online 8 January 2014)

We propose phase shift multiplication effect of all-optical analog to electromagnetically induced transparency in two photonic crystal micro-cavities side coupled to a waveguide system through external optical pump beams. With dynamically tuning the propagation phase of the line waveguide, the phase shift of the transmission spectrum in two micro-cavities side coupled to a waveguide system is doubled along with the phase shift of the line waveguide. π-phase shift and 2π-phase shift of the transmission spectrum are obtained when the propagation phase of the line waveguide is tuned to 0.5π-phase shift and π-phase shift, respectively. All observed schemes are analyzed rigorously through finite-difference time-domain simulations and the coupled-mode formalism. These results show a new direction to the miniaturization and the low power consumption of microstructure integration photonic devices in optical communication and quantum information processing.
[http://dx.doi.org/10.1063/1.4861128]

I. INTRODUCTION

Quantum coherence in atomic systems has led to fascinating and counterintuitive outcomes, such as laser cooling, trapping of atoms, and Bose-Einstein condensates.[1] In electromagnetically induced transparency (EIT), the quantum destructive interference between excitation pathways to the upper level in three-level atomic systems has led to sharp dips of absorption in the medium,[2] resulting in phenomena such as lasing without inversion and freezing light[3] and dynamical storage of light in a solid state system.[4] EIT was originally observed in atomic vapors, yet the narrowness of the EIT window and the complexity of constructing atomic systems restrict the practical use of the EIT effect.[5,6]

To make better use of the EIT effect, classical all-optical EIT-like has been realized on various platforms, including photonic crystal waveguides and micro-cavities,[7] coupled resonance induced transparency (CRIT) systems,[8,9] and plasmonic nanostructures.[10,11] For EIT-like, the narrow transparency peak in the transmission spectrum is associated with a large group delay, which has been experimentally measured in a two-microcavity system.[12] Recently, the different phase shifts of the transmission spectrum in 2-D photonic crystal two micro-cavities have been obtained.[13,14] However, phase shift multiplication effect in two micro-cavities side coupled to a waveguide system is found in our research. This effect can be applied to microstructure integration photonic devices to solve the problems of the high power consumption and the large size.

In this paper, by dynamically tuning the propagation phase of the line waveguide, we demonstrate phase shift multiplication effect which does not require a relatively large average pump power to obtain π-phase shift. The problems of the high power consumption and the large size in microstructure integration photonic devices can be solved, which show a new direction to the miniaturization and the low power consumption of microstructure integration photonic devices in all-optical communication and all-optical signal processing.

The rest of this paper is organized as follows. Section II gives the simplified model to realize EIT-like effect, simulates $|E|^2$ field intensity distributions of coupled-cavity transparency mode, and analyzes the related theory. Section III clarifies phase shift multiplication effect in two micro-cavities side coupled to a waveguide system. Conclusions are given in Sec. IV.

II. EIT-LIKE MODEL DESIGN AND ANALYSIS

This EIT-like system (Fig. 1) consists of a photonic crystal waveguide side-coupled to two photonic crystal cavities. These line-defect-type cavities, with three missing air holes ($L3$) in a triangular-lattice photonic crystal membrane (air hole radius $r = 0.29a_0$, $0.6a_0$ thickness lattice, lattice period a_0 of 420 nm), allow wavelength-scale localization (modal volume $V \sim 0.74(\lambda/n)^3$) for nonlinear and quantum optics.[1,15] In order to increase the bandwidth of the transmission spectrum and avoid the complexity of the experiment, a relatively low intrinsic quality factor ($Q_{\rm int}$) is used in this paper.

When a waveguide is added between two cavities, it would not affect other properties of photonic crystal such as waveguide transmission property. The waveguide is formed by filling one row of air holes along the Γ-K direction. Two cavities are installed on both sides of the waveguide with a distance of three rows of air holes, as shown in Fig. 1.

[a)]Electronic mail: wangtao@hust.edu.cn

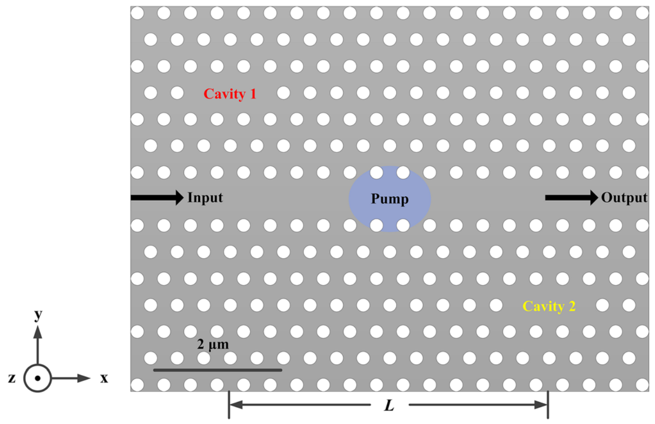

FIG. 1. Schematic of two $L3$-cavities side coupled to a waveguide system, with phase detuning between the cavities. The blue spot indicates the region where the pump beam is focused.

The transparency modes are completely restricted in the cavity because of the photonic crystal gap overlap effect and the cavity mode distribution effect.[16] $|E|^2$ field intensity distributions of the coupled-cavity transparency mode between two $L3$-cavities by 3D-FDTD simulation are shown in Fig. 2. For 3D-FDTD simulation, the index of the silicon slab is set as 3.48 and the mesh order is set as $\lambda/20$. Perfectly matched layer (PML) condition is adopted, and the calculating region is chosen as $50 \times 25a_0$ in x and y directions, respectively. We find that the resonant wavelengths of cavity 1 and cavity 2 are 1563.30 nm [Fig. 2(a)] and 1564.04 nm [Fig. 2(c)], respectively. The transparent wavelength is 1563.67 nm [Fig. 2(b)].

The schematic of the simplified model to realize EIT-like effect by two-cavity side coupled to a waveguide system is shown in Fig. 3.

According to coupled mode theory,[9,17] the dynamic equations for the cavity mode amplitudes are given by the following:

$$\frac{da_1}{dt} = \left[-\frac{1}{2\tau_{tot,1}} + j\omega_1\right]a_1 + \kappa_1 f_{1+} + \kappa_1 f_r, \tag{1a}$$

$$\frac{da_2}{dt} = \left[-\frac{1}{2\tau_{tot,2}} + j\omega_2\right]a_2 + \kappa_2 f_t + \kappa_2 f_{2-}, \tag{1b}$$

where $a_{1,2}$ and $\omega_{1,2}$ denote amplitudes and intrinsic resonant frequencies of each cavity, respectively. $f_{1+,2+}$ and $f_{1-,2-}$ represent amplitudes of input and output waves from input and output ports, respectively. f_t and f_r represent amplitudes of transmission and reflection waves, respectively. They are given by the following equations:

$$f_{1-} = e^{-j\phi} f_r + \kappa_1 a_1, \tag{2a}$$

$$f_t = e^{-j\phi} f_{1+} + \kappa_1 a_1, \tag{2b}$$

$$f_r = e^{-j\phi} f_{2-} + \kappa_2 a_2, \tag{2c}$$

$$f_{2+} = e^{-j\phi} f_t + \kappa_2 a_2. \tag{2d}$$

Coupling coefficients between the cavity and the waveguide are expressed as $\kappa_i = j\exp(-j\phi/2)/(2\tau_{c,i})^{1/2}$ $(i = 1, 2)$, and the phase difference between two cavities is expressed as $\phi = \omega n_{eff} L/c$. Here, ω and n_{eff} are the frequency and the effective refractive index of the waveguide mode, respectively. L is the distance between two cavities. c is the speed of light in free space. The system's round-trip phase also can

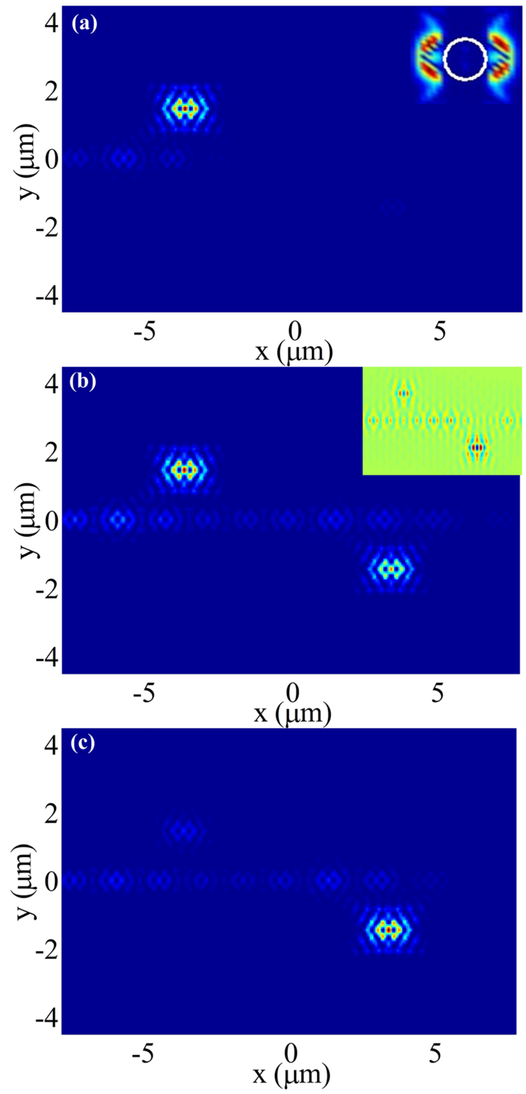

FIG. 2. $|E|^2$ field intensity distributions of the coupled-cavity transparency mode between two $L3$-cavities. (a) The resonant wavelength of cavity 1 is 1563.30 nm. Inset: k-space amplitudes for single $L3$ cavity. (b) The transparent wavelength is 1563.67 nm. Inset: the corresponding E_y field intensity distributions of the transparency mode. (c) The resonant wavelength of cavity 2 is 1564.04 nm.

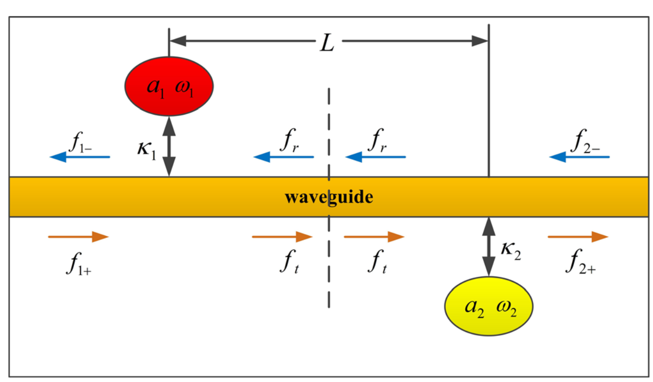

FIG. 3. The schematic of the simplified model to realize EIT-like effect.

be expressed as $\phi = 2n\pi + \Delta\phi$ (where n is an integer). $1/\tau_{c,i}$ is the external loss rate of the waveguide-cavity, relating to the coupling quality factor $Q_{c,i}$ as $1/\tau_{c,i} = \omega/(2Q_{c,i})$, and $1/\tau_{\text{int},i}$ is the intrinsic loss rate, relating to the intrinsic quality factor $Q_{\text{int},i}$ as $1/\tau_{\text{int},i} = \omega/(2Q_{\text{int},i})$. Total decay rates of each cavity $1/\tau_{\text{tot},i}$ can be expressed as $1/\tau_{\text{tot},i=} 1/\tau_{c,i} + 1/\tau_{\text{int},i}$ $(i = 1,2)$. Therefore, we can get the transmission coefficient t as $t = f_{2+}/f_{1+}$ by combining these equations.

For simplicity, we assume that there is only one input light ($f_{2-} = 0$) in the system and two cavities are set as the same optical loss, which means $\kappa_1 = \kappa_2 = \kappa$. So the transmission T and the effective phase shift φ can be calculated as $T = abs\,(t)^2$ and $\varphi = \arg\,(t)$, respectively.

In order to describe phase shift multiplication effect, the refractive index modulation methods that result in the phase shift is discussed. Electric or optical modulation methods relating to the thermo-effect have been adopted in the previous studies. However, the thermo-effect tuning is too slow (the response time at microseconds or even milliseconds) to keep up with fast modulation, all optical signal processing, and optical communication in the future.[17,18] Moreover, at high frequencies, the response is lowered by two orders of magnitude as the nonlinearity is induced by the Kerr effect in silicon (Kerr constant $n_2' \sim 1.0 \times 10^{-12}$ cm^2/W).[18,19] Therefore, free-carrier plasma effect with the response time at picoseconds is applied to improving the tuning rate in this paper. Free carrier mainly comes from two-photon absorption (TPA) effect[20,21] under such ultra-short light pulse. The concentration of free charge in silicon changes both the real and the imaginary parts of the refractive index. According to Kramers-Kronig relations, the relation between the refractive index change and the average pump pulse power P_{avg} at wavelength of 1563.67 nm can be expressed as follow:[22,23]

$$\Delta n = -\left[8.8 \times 10^{-22} \frac{\beta_{TPA} t_p^2}{2\hbar\omega_{pump}\sqrt{\pi} T S^2} P_{avg}^2 + 8.5 \times 10^{-18} \left(\frac{\beta_{TPA} t_p^2}{2\hbar\omega_{pump}\sqrt{\pi} T S^2} P_{avg}^2\right)^{0.8}\right], \quad (3)$$

where ω_{pump} is the frequency of the pump light and $\beta_{TPA} = 7.9 \times 10^{-10}$ cm/W is TPA coefficient. S is the effective area of the pump pulse. The pump light works at a wavelength of 782 nm, which generates pulses with the width $T = 10$ fs at an 80 MHz repetition rate. $t_p = 10$ ps is the pulse duration of the pump light.

The change of the effective refractive index results in the effective phase change of the waveguide signal light when the pump light is focused on the waveguide

$$\Delta\phi = \frac{2\pi}{\lambda} \Delta n_{eff} L', \quad (4)$$

where $\Delta n_{eff} \approx \Delta n$, L' is the length of the pump light in the waveguide region, and λ is the wavelength of the signal light. This modulation method is also suitable for the situation where the photonic crystal waveguide transmits the pump light.

Figure 4 shows the phase shift of the waveguide signal light as a function of the average pump power. The phase shift of the waveguide signal light exhibits a nonlinear trend with the increase of P_{avg}. The phase shifts of the induced signal light are 0.5π and π when the average pump powers are 92.7 mW and 135.5 mW, respectively.

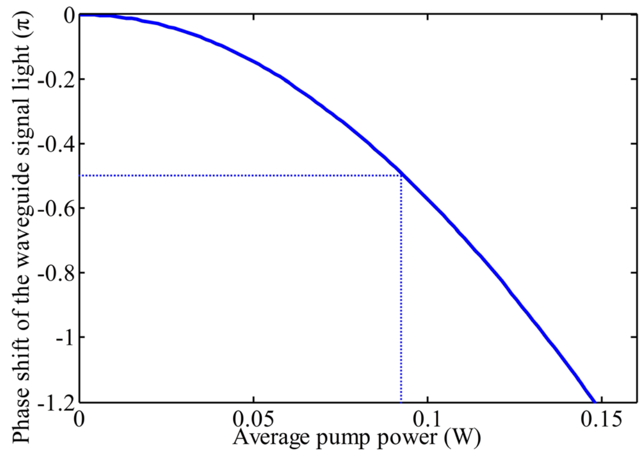

FIG. 4. The phase shift of the waveguide signal light as a function of the average pump power.

III. PHASE SHIFT MULTIPLICATION EFFECT

Controlling of the phase shift of the transmission spectrum is carried out by either tuning the propagation phase of the line waveguide or detuning the resonators' resonant frequencies with a 782 nm pump light focused to a 2.5 μm diameter spot size on the waveguide.[1,15] However, in the case of the same spot size, the resonance detuning mechanism needs a relatively large average pump power to obtain π-phase shift of the transmission spectrum. Therefore, a waveguide phase tuning mechanism is introduced in this paper.

With the progress in dense wavelength division multiplexing (DWDM) and time division multiplexing (TDM), the wide bandwidth of the signal transmission spectrum in optical communication has become an important issue. In order to increase the bandwidth of the signal transmission spectrum, a relatively low Q_{int} is used. The bandwidth of the signal transmission of 0.74 nm is obtained in our research.

When the average pump power is 18 mW, the resonant wavelength of cavity 1 is 1563.30 nm. The strong coupling condition $\gamma \ll |\omega_1 - \omega_2| \ll \gamma_c$ is satisfied when $\Delta\phi = 0$, where γ is the linewidth that is originated from intrinsic cavity losses and γ_c is the linewidth that the microcavity couples to the waveguide, respectively. Two cavities form a large resonant cavity by tuning the distance between two microcavities.

Free-carrier plasma effect reduces the effective refractive index of the line waveguide. As a result, the optical path of the signal light becomes short with the increase of the average pump power. When $P_{avg} > 0$, the phase shift of the waveguide signal light will decrease, so $\Delta\phi < 0$.

Figure 5 shows the normalized transmission intensity spectra and the corresponding phase shift responses under various averages pump powers in two $L3$-cavities side coupled to a waveguide system. In Figs. 5(a) and 5(e), the EIT-like transmission intensity spectra are the same when

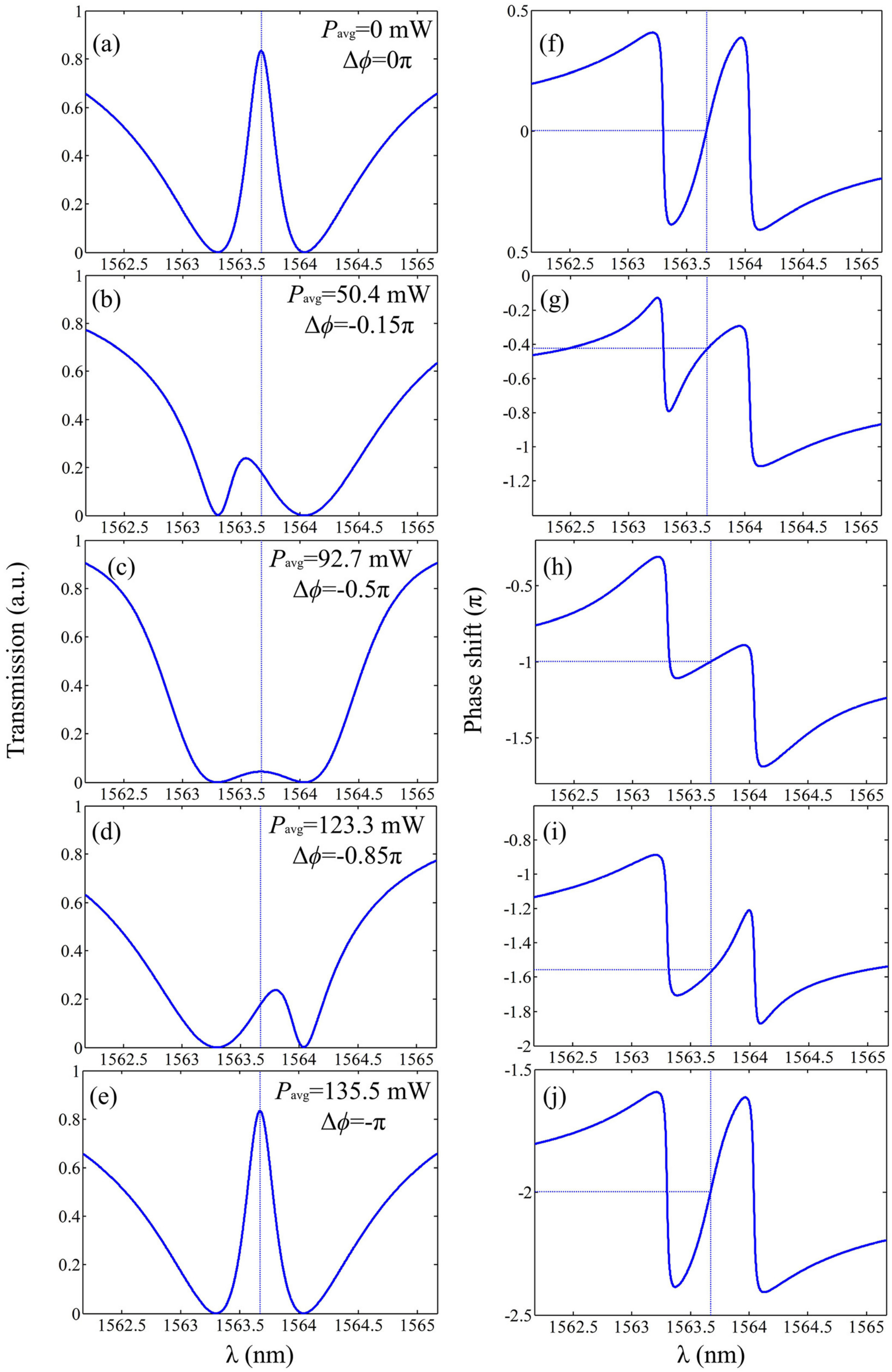

FIG. 5. The normalized transmission intensity spectra and the phase shift responses under different average pump powers in two $L3$-cavities side coupled to a waveguide system. (a)-(e) The EIT-like transmission intensity spectra under various P_{avg}. (f)-(j) The phase shift responses. The intersections of the dashed line represent phase shifts of the transparent wavelength at 1563.67 nm with values of 0π, -0.43π, $-\pi$, -1.57π, and -2π, respectively.

the phase shift of the waveguide signal light is tuned to $-\pi$. The system's round-trip phase is 2π, resulting in a Fabry-Perot resonance. However, the phase shift of the transmission spectrum is changed 2π [from Figs. 5(f) to 5(j)], because free-carrier plasma effect results in the reduction of the effective refractive index of the line waveguide.

When $\Delta\phi \in [0,-0.5\pi)$, the EIT-like transmission window is blue-shifted and the transmission intensity is reduced

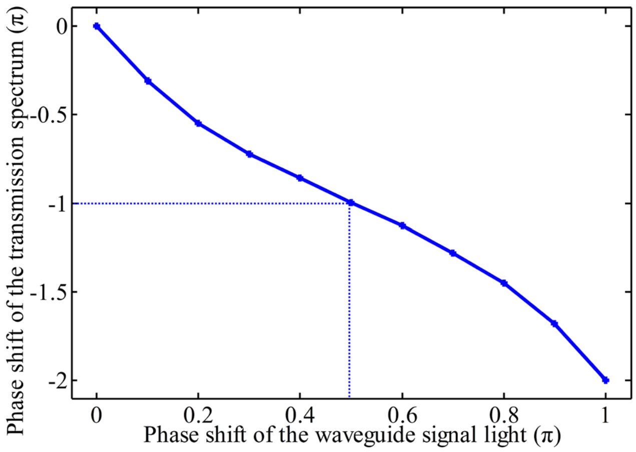

FIG. 6. Phase shifts of the transmission spectrum at the transparent wavelength of 1563.67 nm as a function of phase shifts of the waveguide signal light.

by 70.24% compared with Fig. 5(a), as shown in Figs. 5(a) and 5(b). However, when $\Delta\phi \in [-0.5\pi, -\pi)$, the EIT-like transmission window is red-shifted and the transmission intensity is increased, as shown in Figs. 5(c) and 5(d). In Figs. 5(b) and 5(d), the round-trip phase is tuned away from 2π, resulting in asymmetric Fano-like transmission spectra. When $\Delta\phi = -0.5\pi$, the coupling strength between two cavities is the weakest with the minimum value in the transmission spectrum [Fig. 5(c)], which results from the dissatisfaction of Fabry-Perot resonance condition of the waveguide phase. It is important to note that the corresponding phase shift values of the transparent wavelength at 1563.67 nm are 0π, -0.43π, $-\pi$, -1.57π, and -2π, respectively [Figs. 5(f)–5(j)].

Figure 6 shows the relation between the phase shift of the waveguide signal light and the phase shift of the transmission spectrum at the transparent wavelength of 1563.67 nm. Phase shifts of the transmission spectra are zero and $-\pi$ when phase shifts of the line waveguide $\Delta\phi$ are zero and 0.5π, respectively. Apparently, π-phase shift and 2π-phase shift of the transmission spectrum are obtained when the propagation phase of the line waveguide is tuned to 0.5π-phase shift and π-phase shift, respectively, as shown in Fig. 6. Therefore, phase shift multiplication effect is found in two $L3$-cavities side coupled to a waveguide system. The effect does not require a relatively large average pump power to obtain π-phase shift. Hence the power consumption of microstructure integration photonic devices can be reduced. Moreover, phase shift multiplication effect is also suitable for microstructure integration photoelectronic devices with electric or optical modulation methods relating to the thermo-effect.

IV. CONCLUSIONS

In conclusion, we propose phase shift multiplication effect of all-optical EIT-like in two photonic crystal micro-cavities side coupled to a waveguide system. The effect does not require a relatively large average pump power to obtain π-phase shift. Moreover, it is suitable for microstructure integration photoelectronic devices with various modulation methods such as free-carrier plasma effect modulation and Kerr effect modulation. The effect can reduce the power consumption of microstructure integration photonic devices by using the low average pump power in two micro-cavities side coupled to a waveguide system. This research shows a new direction to the miniaturization and the low power consumption of microstructure integration photonic devices in all-optical communication and all-optical signal processing.

ACKNOWLEDGMENTS

This work was supported by the National Natural Science Foundation of China (Grant No. 61376055) and the National Basic Research Program of China (Grant No. 2010CB923204).

[1]X. Yang, M. Yu, D.-L. Kwong, and C. W. Wong, Phys. Rev. Lett. **102**, 173902 (2009).
[2]S. E. Harris, Phys. Today **50**(7), 36 (1997).
[3]L. V. Hau, S. E. Harris, Z. Dutton, and C. H. Behroozi, Nature (London) **397**, 594 (1999).
[4]J. J. Longdell, E. Fraval, M. J. Sellars, and N. B. Manson, Phys. Rev. Lett. **95**, 063601 (2005).
[5]L. Zhou, T. Ye, and J. Chen, Opt. Lett. **36**, 13 (2011).
[6]Z. Zou, L. Zhou, X. Sun, J. Xie, H. Zhu, L. Lu, X. Li, and J. Chen, Opt. Lett. **38**, 1215 (2013).
[7]J. Pan, Y. Huo, S. Sandhu, N. Stuhrmann, M. L. Povinelli, J. S. Harris, M. M. Fejer, and S. Fan, Appl. Phys. Lett. **97**, 101102 (2010).
[8]Q. Xu, S. Sandhu, M. L. Povinelli, J. Shakya, S. Fan, and M. Lipson, Phys. Rev. Lett. **96**, 123901 (2006).
[9]Q. Li, T. Wang, Y. Su, M. Yan, and M. Qiu, Opt. Express **18**, 8367 (2010).
[10]J. Chen, C. Wang, R. Zhang, and J. Xiao, Opt. Lett. **37**, 5133 (2012).
[11]H. Lu, X. Liu, and D. Mao, Phys. Rev. A **85**, 053803 (2012).
[12]Q. Xu, J. Shakya, and M. Lipson, Opt. Express **14**, 6463 (2006).
[13]G. Lenz, B. J. Eggleton, C. K. Madsen, and R. E. Slusher, IEEE J. Quantum Electron. **37**, 525 (2001).
[14]Y. Huo, S. Sandhu, J. Pan, N. Stuhrmann, M. L. Povinelli, J. M. Kahn, J. S. Harris, M. M. Fejer, and S. Fan, Opt. Lett. **36**, 1482 (2011).
[15]X. Yang, M. Yu, D.-L. Kwong, and C. W. Wong, IEEE J. Sel. Top. Quantum Electron. **16**, 288 (2010).
[16]P. R. Villeneuve, S. Fan, and J. D. Joannopoulos, Phys. Rev. B **54**, 7837 (1996).
[17]H. A. Haus, *Waves and Fields in Optoelectronics* (Prentice-Hall, Englewood Cliffs, NJ, 1984).
[18]K. Inoue, H. Oda, N. Ikeda, and K. Asakawa, Opt. Express **17**, 7206 (2009).
[19]V. Eckhouse, I. Cestier, G. Eisenstein, S. Combrie, G. Lehoucq, and A. De Rossi, Opt. Express **20**, 8524 (2012).
[20]F. R. Laughton, J. H. Marsh, and J. S. Roberts, Appl. Phys. Lett. **60**, 166 (1992).
[21]C. Manolatou and M. Lipson, IEEE J. Lightwave Technol. **24**, 1433 (2006).
[22]R. A. Soref and B. R. Bennett, Proc. SPIE **0704**, 32 (1986).
[23]R. A. Soref and B. R. Bennett, IEEE J. Quantum Electron. **23**, 123 (1987).